VIP Functionalized Nanoparticles

DOI: 10.1002/anie.201203193

# Imageable Antigen-Presenting Gold Nanoparticle Vaccines for Effective Cancer Immunotherapy In Vivo**

*In-Hyun Lee, Ho-Keun Kwon, Sukyung An, Daejin Kim, Sunghyun Kim, Mi Kyung Yu, Jae-Hyuk Lee, Tae-Sup Lee, Sin-Hyeog Im, and Sangyong Jon**

Vaccination with the aid of adjuvants is a highly effective therapeutic option for the prevention of various diseases.[1] However, development of vaccines against existing cancers and chronic viral diseases, such as hepatitis C and HIV, has proved difficult owing in large part to an inability to induce concerted and potent humoral and cellular immunity.[2] With the aim of overcoming this problem, much effort has gone into developing novel technologies for therapeutic cancer vaccines that enable long-lasting induction of strong, antigen-specific $CD8^+$ T cells, as well as induction of antibody responses to existing tumors.[3] A key consideration in developing such technology is how to achieve efficient antigen delivery to antigen-presenting cells (APCs) with subsequent activation and maturation of cells that maximize cross-presentation for inducing cytotoxic $CD8^+$ T cell responses.[4] In that sense, vaccine delivery to a local lymph node (LN) might be an appropriate strategy, because the node would contain a high population of APCs (e.g., resident dendritic cells, plasmacytoid dendritic cells, and macrophages) along with immune cells responsible for both humoral and cellular immunity.[5] To that end, nanoparticles of natural or synthetic origin have emerged as potential candidates for antigen delivery,[6] since they can be efficiently delivered to LNs through lymphatic vessels in a size-dependent manner.[5b,7] Importantly, smaller nanoparticles (ca. 25 nm in diameter) could lead to significantly larger accumulation in a local LN than larger nanoparticles of approximately 100 nm in size.[5b]

There are four key considerations when designing a nanoparticulate vaccine for targeting LNs: 1) for efficient delivery, the particle diameter should be below 50 nm; 2) the antigens and/or adjuvants should be versatile and easily accommodated to the nanoparticles; 3) after internalization, the vaccine must properly activate APCs to facilitate induction of humoral and cellular immunity; and 4) it is beneficial if the vaccine is traceable in a noninvasive manner to predict efficacy. For the following reasons, gold nanoparticles (AuNPs) may be one of the most suitable nanoparticles for the purpose. First, it is easy to control the size of AuNPs, which can range from approximately 1 nm to several hundred nm. Second, a variety of molecular species, including proteins,[8] peptides,[9] and oligonucleotides,[10] can be easily attached to the surface of AuNPs using simple chemistry. Third, AuNPs are biocompatible and nontoxic.[8b,d] Fourth, AuNPs can be tracked using computed tomography (CT) imaging, which is readily available at nearly all hospitals.[10,11] With these considerations in mind, herein we, for the first time, report AuNP-based cancer vaccines that enable efficient delivery of an antigen to target LNs, tracking of the vaccines using noninvasive clinical imaging, and effective cancer prevention and therapy.

Scheme 1 shows a schematic illustration of the preparation of an AuNP-based vaccine. To optimize delivery to target LNs, we synthesized AuNPs with diameters of approximately 7 nm. Red fluorescent protein (RFP) was chosen as a model antigen and was engineered to have two additional cysteines at its C terminus; this modification facilitated conjugation to the surface of AuNPs through formation of an Au–S bond. Finally, a thiol-modified CpG 1668 oligodeoxynucleotide (ODN; CpG 1668 is an ODN that contains CpG motifs) with a spacer consisting of ten adenine nucleotides ($A_{10}$) was also conjugated to the RFP/AuNP, because CpG 1668 is known to strongly stimulate immune responses through activation of toll-like receptor 9 (TLR-9). We observed that

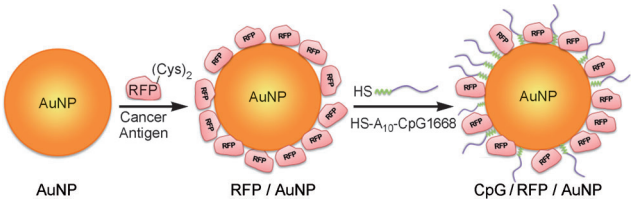


***Scheme 1.*** Schematic representation of the preparation of an RFP/AuNP and an CpG/RFP/AuNP.

[*] I.-H. Lee, S. An, D. Kim, S. Kim, M. K. Yu, Prof. S. Jon
Biological Science Department
Korea Advanced Institute of Science and Technology (KAIST)
291 Daehak-ro,Yuseong-gu, Daejeon 305-701 (South Korea)
E-mail: syjon@kaist.ac.kr
H. K. Kwon, Prof. S.-H. Im
School of Life Sciences
Gwangju Institute of Science and Technology (GIST)
123 Cheomdangwagi-ro, Gwangju 500-712 (South Korea)
Prof. J.-H. Lee
Department of Pathology
Jeonnam National University Medical School
5 Hak1-dong, Gwangju 501-746, (South Korea)
Dr. T.-S. Lee
Molecular Imaging Research Center
Korea Institute of Radiological and Medical Sciences (KIRAMS)
215-4 Gongneung-Dong, Nowon-Gu, Seoul 139-706 (South Korea)

[**] This study was supported by the Converging Research Center Program through the National Research Foundation of Korea (NRF) funded by the Ministry of Education, Science and Technology (grant number: 2011K000797 and 20120006074) and by a grant from Cell Dynamics Research Center, NRF (grant number: 20120000771).

Supporting information for this article is available on the WWW under http://dx.doi.org/10.1002/anie.201203193.

the modified CpG ODN could produce a level of immune stimulation similar to that of an original CpG 1668 ODN (Figure S1 in the Supporting Information). After each conjugation step, the size of the resultant RFP/AuNP ((14 ± 3) nm) and the CpG/RFP/AuNP ((23 ± 7) nm) was increased compared to the bare AuNP ((7 ± 2) nm; Figure S2e in the Supporting Information). Furthermore, there was a slight shift in the characteristic absorbance spectrum of the particle with increasing size (Figure S2f in the Supporting Information). Protein assays showed the antigen concentration to be approximately 1.5 μg RFP/pmol AuNP (ca. 54 RFPs per AuNP) on RFP/AuNPs and approximately 1 μg RFP/pmol AuNP (ca. 36 RFPs per AuNP) on CpG/RFP/AuNPs.

Moreover, ODN assays using Quant-iT™OliGreen ssDNA reagent revealed that approximately 318 ng CpG ODN/pmol AuNP (ca. 32 ODNs per AuNP) was immobilized on the CpG/RFP/AuNPs. Together, these data confirm the successful conjugation of RFP and CpG ODN to the surface of AuNPs. Furthermore, the stability test of conjugated RFP on AuNPs under physiologically relevant reducing environments (20 μM of glutathione) suggested that more than 80% of initial RFP antigen on AuNPs could be delivered to the target LN (Figure S3 in the Supporting Information).

We initially examined how efficiently our AuNP-based cancer vaccines could be delivered to local LNs. RFP/AuNPs or CpG/RFP/AuNPs dispersed in saline were injected into the right rear footpads of mice, after which the location of the AuNPs was monitored with CT imaging for up to seven days. Two days after injection, we observed a bright signal at the boundary of the popliteal LN, which is the node nearest the injected footpad, thus indicating that the AuNP vaccines were efficiently delivered to the target LN (Figure 1a). The delivered AuNPs were still present at the node seven days after injection (Figure S4d in the Supporting Information); moreover, the accumulated AuNP vaccine was clearly visible as a dark band within collected popliteal LNs ($n = 3$; Figure 3b). We then used inductively coupled plasma–atomic emission spectroscopy (ICP–AES with a detection limit of 0.02 μg $L^{-1}$) to measure the AuNP concentrations within the popliteal and neighboring superficial lingual LNs at various times after injection of the RFP/AuNPs. A substantial fraction of the nanoparticles ((64.1 ± 16.6)% of the initial dose) was detected in the popliteal LN, and a small portion was also found in the neighboring superficial lingual LNs (Figure S5 in the Supporting Information). That the portion in the lingual LNs increased somewhat over time suggests the AuNPs traveled from the popliteal node to the secondary superficial lingual nodes; this movement may be advantageous for augmenting the potential encounter between the nanoparticle vaccines and APCs. Critical issues in that regard are where nanoparticle vaccines are delivered within the target LN and what types of APCs take up the antigen-carrying nanoparticles. Histological examination of silver-stained tissues showed that both RFP/AuNPs and CpG/RFP/AuNPs were initially delivered to the subcapsular sinus region of the popliteal LN through an afferent lymphatic pathway (Figure 1c and Figure S6 in the Supporting Information), and then they moved to the paracortex (T cell zone) region; this finding correlates well with the CT imaging data.

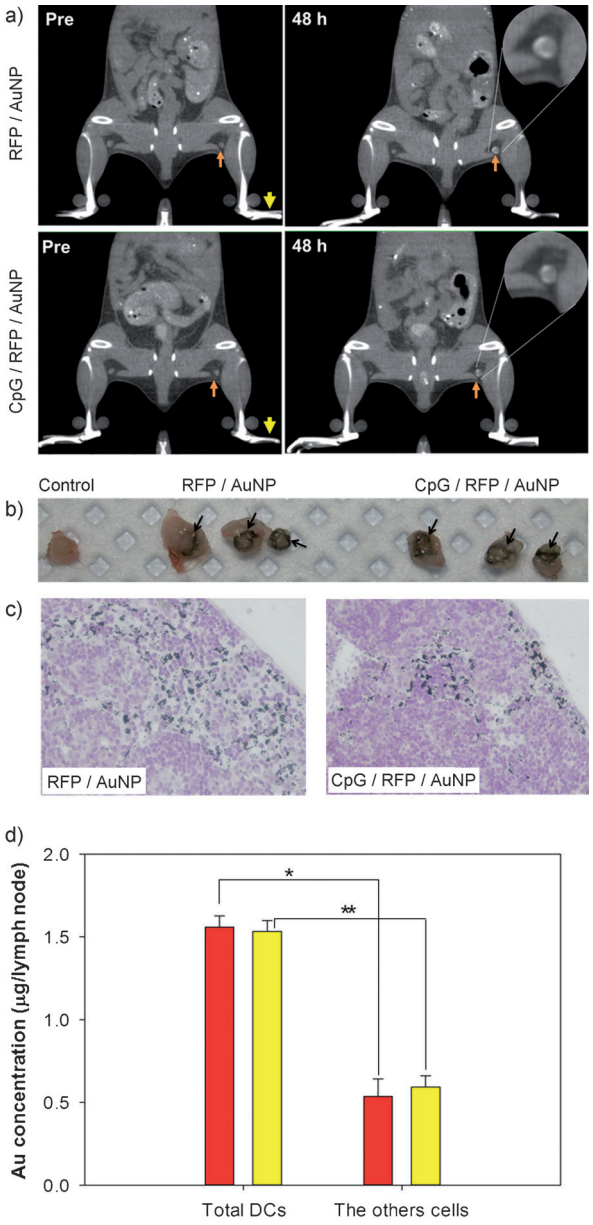


***Figure 1.*** a) CT images obtained before (Pre) and 48 h after injection of RFP/AuNPs or CpG/RFP/AuNPs into the right rear footpad (yellow arrow). We observed the right popliteal LN (golden arrow) after injection. b) Optical images of the dissected popliteal lymph nodes taken 48 h after injection of RFP/AuNP and CpG/RFP/AuNP vaccines. c) Silver-stained sections of the right popliteal LN confirm the presence of RFP/AuNPs and CpG/RFP/AuNPs. d) Graph showing AuNP (Au) levels in total DCs and the others cells within the right popliteal LN (*$P < 0.05$, **$P < 0.005$ between two groups) after injection with RFP/AuNPs (red bars) or CpG/RFP/AuNPs (yellow).

We also examined whether the delivered AuNP-based vaccines were taken up by APCs in the target LN. Two days after footpad injection of RFP/AuNPs or CpG/RFP/AuNPs, we isolated total lymphocytes from popliteal LNs and then used ICP–AES to measure the AuNP fractions within the dendritic cells (DCs; i.e., plasmacytoid and classical DCs) and

  

other cell populations (Figure 1d). We found that the DCs contained a significantly larger fraction of the delivered Au than the other lymphocytes, despite the fact that DCs account for only a small fraction of lymphocytes present in the LN (ca. 1% constitution).[12] This selective and significant delivery of AuNP-based vaccine to DCs is promising, as DCs play a key role in antigen presentation and subsequent communication with immune cells to induce humoral and cellular immunity.[4b,5b,13] Notably, the accumulation of our AuNP-based vaccine in DCs was closely related to the localization of DCs in the LNs. The first location to which DCs migrate within LNs is reportedly the subcapsular sinus of the afferent lymph-node hemisphere,[14] which is also where our AuNP-based vaccines accumulate. Together, these results demonstrate that our AuNP-based vaccines can be successfully delivered to APCs (mostly DCs) in target LNs and that they can be tracked or monitored by using CT imaging.

We next determined whether AuNP-based vaccines delivered to the popliteal LN could elicit antigen-specific immune responses. After immunizing groups of mice with RFP alone, RFP/AuNPs, or CpG/RFP/AuNPs, levels of RFP-specific immunoglobin G (IgG) were measured in serum using an enzyme-linked immunosorbent assay (ELISA). For comparison, a mixture of RFP and alum ((3359 ± 630) nm in size) was used as an example of a conventional particle-based vaccine.[15]

High levels of RFP-specific IgG were observed in all mice treated with different nanoparticles (RFP/AuNPs, CpG/RFP/AuNPs, and Alum-RFP mixture; Figure 2a), whereas levels of the specific antibody were three orders of magnitude lower following immunization with RFP alone. Antibody isotyping revealed that both AuNP-based vaccines primarily induced Th1-driven immune responses, whereas the Alum-RFP mixture stimulated a Th2-driven response (Figure S7a in the Supporting Information). This result is in good agreement with earlier reports[5a,16] and suggests that our AuNP-based vaccines are delivered directly to the target LNs; that is, they are not taken up by peripheral DCs at the injection site that then move to the target LN, as is the case with the Alum-RFP mixture. Interestingly, the RFP-specific IgG titers in the group immunized with RFP/AuNPs (adjuvant-free) were similar to those in the group immunized with CpG/RFP/AuNPs. Although the mechanism for immune stimulation by antigen-bearing AuNPs remains unclear, Puntes and co-workers reported that AuNPs conjugated to repetitive and homogenous antigens were able to stimulate immune responses in an in vitro setting, even without adjuvants.[9] In a preliminary experiment, we observed that RFP/AuNPs could stimulate activation of an alternative complement (that is, cleavage of complement component C3 to C3a and C3b; Figure S8 in the Supporting Information). We therefore speculate that similar complement activation may be responsible for activation and maturation of APCs such as DCs in an in vivo setting.

We also assessed changes in the populations of naïve and regulatory T (Treg) cells in the popliteal LN after immunization with RFP/AuNPs or CpG/RFP/AuNPs (Figure S9 in the Supporting Information). We found that the naïve T cell population was substantially reduced, but there was little change in the Treg cell population, which suggests our AuNP-based vaccine may work through conversion of naïve to activated T cells. To investigate antigen-specific T cell proliferation, which is an important index for evaluating vaccination efficacy, we first immunized mice, then isolated T cells from the popliteal and superficial lingual LNs, and finally treated these cells with α-chymotrypsinized RFP. Both groups

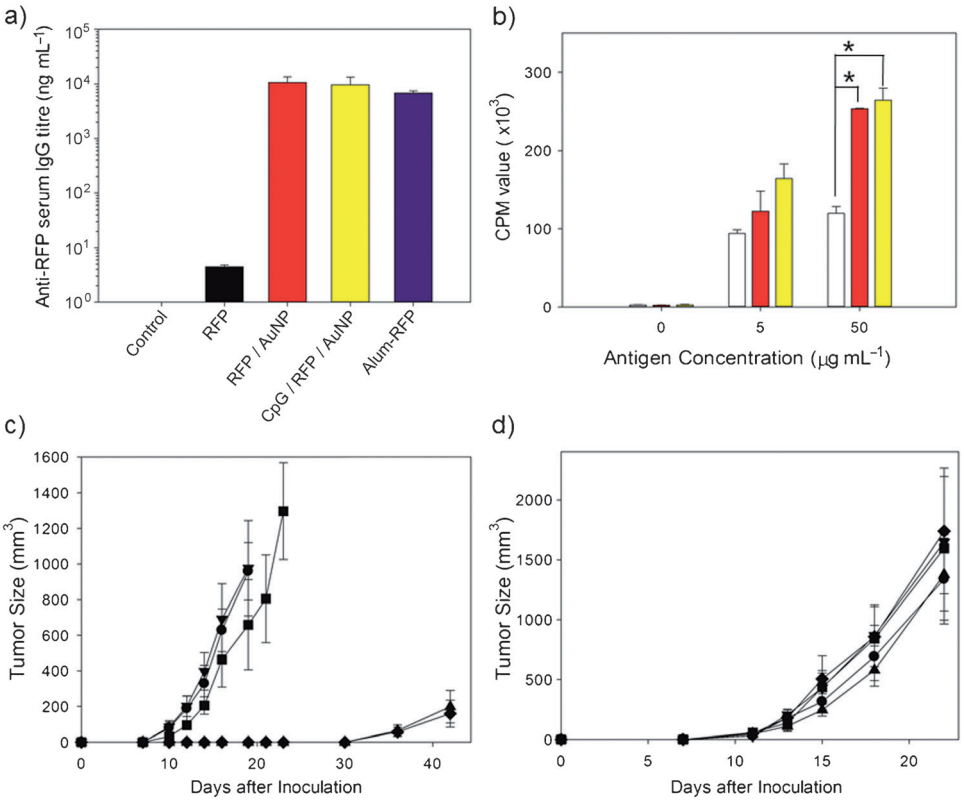


***Figure 2.*** In vivo anticancer efficacy of AuNP-based cancer vaccines. a) RFP-specific IgG titers after immunization with PBS (control), Alum-RFP mixture, RFP/AuNPs, or CpG/RFP/AuNPs. b) T cell proliferation following antigen stimulation. T cells were isolated from mice immunized three times with PBS (control, white bars), RFP/AuNPs (red), or CpG/RFP/AuNPs (yellow). CPM = counts per minute. c, d) Changes in the size of the tumor consisting of RFP-expressing B16F10 cells (c), or wild-type B16F10 cells (d) after immunization with PBS (control, ●), AuNPs (▼), RFP (■), RFP/AuNPs (◆), CpG/RFP/AuNPs (▲). (*$P < 0.05$ between two groups).

immunized with RFP/AuNPs and CpG/RFP/AuNPs exhibited antigen-specific T cell proliferation that was much higher than in the control (PBS) group; moreover, the magnitude of the increase was proportional to the dose of the antigen (Figure 2b). These results indicate that RFP/AuNPs and CpG/RFP/AuNPs can not only convert naïve T cells to active ones, but they can also facilitate T cell proliferation in an antigen-specific manner after LN targeting.

Our finding that both RFP/AuNPs and CpG/RFP/AuNPs elicited high levels of antigen-specific antibody production and T cell proliferation prompted us to test whether they could also prevent tumor formation in vivo. RFP-expressing B16F10 murine melanoma cells were used to prepare a mouse tumor model, and RFP expression and tumor growth were confirmed by fluorescence imaging (Figure S10 in the Supporting Information). For vaccination, we injected the footpads of C57Bl/6 mice three times at one week intervals with PBS, RFP, AuNPs, RFP/AuNPs, or CpG/RFP/AuNPs before inoculation of the RFP-expressing cancer cells. Both RFP/AuNPs and CpG/RFP/AuNPs effectively prevented tumor growth for up to four weeks after cancer inoculation, thereby significantly increasing survival rates, compared to mice injected with the control (Figure 2c and Figure S7b in the Supporting Information). Vaccination with free RFP failed to inhibit tumor growth, and also AuNP-based vaccine did not prevent tumor formation from wild-type B16F10 cells, which do not express the RFP antigen (Figure 2d). Thus our AuNP-based vaccines only exerted effects against tumors presenting a specific antigen.

We then tested whether the AuNP-based vaccines would prevent cancer metastasis in a lung metastasis model. The extent of the lung metastasis was determined based on the RFP fluorescence signal. Also, we investigated tumor nodules in lung and lung weight. These experiments on in vivo prevention of metastasis showed that RFP/AuNPs and CpG/RFP/AuNPs successfully prevented lung metastasis by inducing a potent immune response driven by Th1 helper T cells (Figure S11 in the Supporting Information).

When used in clinical settings, the practical aim of cancer vaccines is to effectively cure or at least inhibit the growth of existing tumors. To achieve that aim it is necessary to use a strong adjuvant in conjunction with a cancer-specific antigen so that robust humoral and cellular immunity is induced. CpG ODNs have been used previously as adjuvants for cancer vaccines[3,17] and are known to enhance B and T cell responses to cancer antigens through TLR9 activation.[17b,c,18] However, we observed that there was little difference in the efficacy of RFP/AuNPs and CpG/RFP/AuNPs in earlier tumor prevention and metastasis models, despite lack of an adjuvant in the RFP/AuNP group. We had hypothesized that conjugation of a potent CpG ODN adjuvant to the AuNP surface (CpG/RFP/AuNP) would enable the vaccine to potentiate or facilitate cytotoxic T cell (CTL)-based cellular immunity more efficiently, thus leading to better therapeutic outcomes against existing tumors. To further test that hypothesis, we estimated the therapeutic efficacy of the AuNP-based vaccines on existing tumors in vivo. Once tumors had reached approximately 40 $mm^3$ in size (on day ten after inoculation), we injected the footpads of the mice five times with PBS, RFP, AuNPs, RFP/AuNPs or CpG/RFP/AuNPs according to a predetermined schedule (arrows in Figure 3a). In the groups treated with RFP/AuNPs and CpG/RFP/AuNPs, tumor growth was substantially slower than in the other groups. Furthermore, the antitumor efficacy of CpG/RFP/AuNPs was significantly greater than that of RFP/AuNPs ($p < 0.05$). This difference in the antitumor activity is likely attributable to the lack of a CpG ODN adjuvant on the RFP/AuNPs.

To evaluate the effect of the CpG adjuvant on therapeutic efficacy against an existing tumor model in more detail, we investigated the lymphocytic expression of IFN-γ, which activates natural killer (NK) cells and is responsible for the Th1 response and antitumor properties of cancer vaccines, and the activation of antigen-specific $CD8^+$ cytotoxic T cells. After three immunizations with PBS, RFP, RFP/AuNPs, or CpG/RFP/AuNPs, total lymphocytes were isolated from the popliteal LNs and stimulated with phytohemagglutinin (PHA; positive control), α-chymotrypsinized RFP (Antigen), and PBS (negative control). Then, expression of IFN-γ and its secretion from the stimulated lymphocytes were assessed using fluorescence-activated cell sorting (FACS) analysis (Figure S12 in the Supporting Information) and an ELISA (Figure 3b), respectively. As expected, PHA stimulated high levels of IFN-γ secretion in all four immunization groups, whereas PBS elicited no increases in secretion above baseline. Among the three groups that were treated with the RFP antigen, we confirmed notable increases in IFN-γ secretion from lymphocytes in the groups that were immunized with RFP/AuNPs and CpG/RFP/AuNPs, whereas lymphocytes in the group immunized with RFP secreted only basal levels of IFN-γ. These results indicate that our AuNP-based vaccines strongly stimulate IFN-γ secretion by lymphocytes through antigen-specific pathways. Moreover, immunization with CpG/RFP/AuNPs led to greater IFN-γ expression and secretion than immunization with RFP/AuNP; we suggest this finding reflects the presence of the adjuvant in CpG/RFP/AuNPs. We next tested whether the AuNP-based vaccines would induce the proliferation and activation of antigen-specific $CD8^+$ cytotoxic T cells (CTLs). Primary lymphocytes isolated from the popliteal LN after three immunizations with PBS, RFP, RFP/AuNPs, or CpG/RFP/AuNPs were stimulated with various concentrations of RFP antigen (0–50 $\mu g\,mL^{-1}$). Then after 24 h we double stained the lymphocytes using anti-CD8 and anti-granzyme B (GZMB) antibodies for FACS analysis (Figure 3c). GZMB is released by the cytoplasmic granules from CTLs and NK cells,[19] and can induce apoptosis in cancer and virus-infected cells. The FACS data showed that the $CD8^+$ CTL population increased significantly with increasing antigen concentration in both groups immunized with RFP/AuNPs and CpG/RFP/AuNPs, though the effect was more pronounced in the latter. By contrast, there was little change in the $CD8^+$ CTL populations in the groups immunized with PBS and RFP. This result suggests that the greater antitumor efficacy of the CpG/RFP/AuNP vaccine may reflect the ability of CpG ODN adjuvant to efficiently stimulate the proliferation of $CD8^+$ CTLs and production of anticancer materials (IFN-γ and GZMB).[17b,c,18b]

In summary, vaccines against cancers and chronic viral diseases should induce potent humoral immune responses as

  

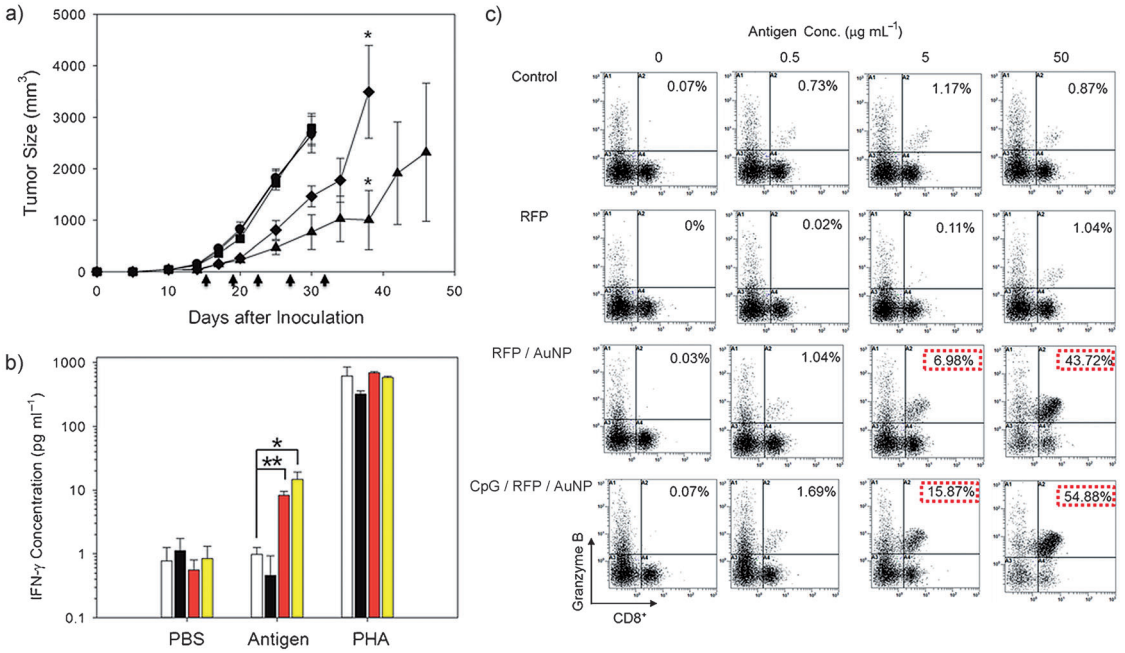


***Figure 3.*** AuNP-based vaccines inhibit growth of solid tumors. a) Mice were subcutaneously inoculated with RFP-expressing B16F10 cells on day 0. The mice were immunized with five injections of PBS (control, ●), AuNPs (▼), RFP (■), RFP/AuNPs (◆), or CpG/RFP/AuNPs (▲) according to the schedule (arrows). b) Analysis confirming the adjuvant effect of AuNP-based vaccines through RFP-specific immune responses. Total lymphocytes were isolated from the mice that were immunized with PBS (white bars), RFP (black), RFP/AuNPs (red), or CpG/RFP/AuNPs (yellow), as described in the Supporting Information. After stimulation with PBS, Antigen, or PHA, interferon-γ (IFN-γ) production was measured by using an ELISA. c) RFP-specific $CD8^+$ T cell activation. Mice were immunized as described in the Supporting Information. After isolation of total lymphocytes, these were stimulated with the indicated RFP antigen concentration. Double positive cells ($CD8^+$ granzyme $B^+$) were then identified, and the ratios of the $CD8^+$ granzyme $B^+$ cell fractions are shown (*$P < 0.05$, **$P < 0.005$ between two groups).

well as cytotoxic T cell responses.[1c,d,2a,16,20] Nanoparticulate carriers that mimic viral properties in terms of size, geometry, and antigen display, may be appropriate candidates for induction of such responses.[3,21] Their size enables them to reach local LNs directly and interact with APCs to trigger antigen-specific immune responses. Furthermore, linkage of TLR ligands to antigen-displaying nanoparticles can effectively lead to activation of DCs engulfing nanoparticulate vaccines and facilitate induction of T cell responses.[17] In this regard, we showed that a AuNP-based antigen carrier system could potentially serve as a vaccine for cancer prevention and treatment. AuNPs displaying RFP as a model antigen and CpG ODN as a TLR9 ligand reached target LNs, where they interacted with DCs, thereby potently inducing antibody production through a Th1-driven pathway and priming CTL responses in an antigen-specific manner. As a result, AuNP-based vaccines exhibited significant antitumor efficacy in RFP-expressing melanoma tumor models. AuNPs have several advantages over other nanoparticulate-based carriers. First, it is easy to precisely control the size of AuNPs for different applications. Second, a variety of antigens and adjuvants can be easily linked to and displayed on their surface, thus suggesting AuNP-based vaccines could be used to treat diseases other than cancer. Third, AuNP-based vaccines can be detected or tracked using noninvasive CT imaging, providing clinicians with information on where or whether the vaccines have been delivered, which would help to predict or evaluate therapeutic efficacy. Finally, there would be less safety issues with AuNP-based vaccines compared to other nanoparticles, as AuNPs are known to be biocompatible and nontoxic. Taken together, these findings suggest AuNP-based antigen delivery systems may be a useful vaccine technology able to prevent and/or treat a variety of ailments.

Received: April 25, 2012
Published online: July 29, 2012

**Keywords:** cancer therapy · computed tomography · nanoparticles · immunology · vaccines

[1] a) R. Rappuoli, C. W. Mandl, S. Black, E. D. Gregorio, *Nat. Rev. Immunol.* **2011**, *11*, 865–872; b) S. Pejawar-Gaddy, O. J. Finn, *Crit. Rev. Oncol. Hematol.* **2008**, *67*, 93–102; c) J. A. Berzofsky, M. Terabe, S. Oh, I. M. Belyakov, J. D. Ahlers, J. E. Janik, J. C. Morris, *J. Clin. Invest.* **2004**, *113*, 1515–1525; d) T. H. Schreibera, L. Raezc, J. D. Rosenblatt, E. R. Podack, *Semin. Immunol.* **2010**, *22*, 105–112.

[2] a) J. J. Moon, H. Suh, A. Bershteyn, M. T. Stephan, H. Liu, B. Huang, M. Sohail, S. Luo, S. H. Um, H. Khant, J. T. Goodwin, J. Ramos, W. Chiu, D. J. Irvine, *Nat. Mater.* **2011**, *10*, 243–251; b) T. Mamo, E. A. Moseman, N. Kolishetti, C. Salvador-Morales, J. Shi, D. R. Kuritzkes, R. Langer, U. v. Andrian, O. C. Farokhzad, *Nanomedicine* **2010**, *5*, 269–285.

[3] M. F. Bachmann, G. T. Jennings, *Nat. Rev. Immunol.* **2010**, *10*, 787–796.

  

[4] a) R. W. Hung, S. Hamdy, A. Haddadi, Z. Ghotbi, A. Lavasanifar, *Curr. Drug Delivery* **2011**, *8*, 274 – 281; b) A. H. Samar Hamdy, Z. Ghotbi, R. W. Hung, A. Lavasanifar, *Curr. Drug Delivery* **2011**, *8*, 261 – 273.
[5] a) D. Mohanan, B. Slütter, M. Henriksen-Lacey, W. Jiskoot, J. A. Bouwstra, Y. Perrie, T. M. Kündig, B. Gander, P. Johansen, *J. Controlled Release* **2010**, *147*, 342 – 349; b) S. T. Reddy, A. J. v. d. Vlies, E. Simeoni, V. Angeli, G. J. Randolph, C. P. O'Neil, L. K. Lee, M. A. Swartz, J. A. Hubbell, *Nat. Biotechnol.* **2007**, *25*, 1159 – 1164.
[6] a) M. Skwarczynski, M. Zaman, C. N. Urbani, I.-C. Lin, Z. Jia, M. R. Batzloff, M. F. Good, M. J. Monteiro, I. Toth, *Angew. Chem.* **2010**, *122*, 5878 – 5881; *Angew. Chem. Int. Ed.* **2010**, *49*, 5742 – 5745; b) M. Wei, N. Chen, J. Li, M. Yin, L. Liang, Y. He, H. Song, C. Fan, Q. Huang, *Angew. Chem.* **2012**, *124*, 1228 – 1232; *Angew. Chem. Int. Ed.* **2012**, *51*, 1202 – 1206; c) B. G. De Geest, M. A. Willart, B. N. Lambrecht, C. Pollard, C. Vervaet, J. P. Remon, J. Grooten, S. D. Koker, *Angew. Chem.* **2012**, *124*, 3928 – 3932; *Angew. Chem. Int. Ed.* **2012**, *51*, 3862 – 3866; d) Y.-W. Noh, Y.-S. Jang, K.-J. Ahn, Y. T. Lim, B. H. Chung, *Biomaterials* **2011**, *32*, 6254 – 6263.
[7] a) M. A. Swartz, *Adv. Drug Delivery Rev.* **2001**, *50*, 3 – 20; b) C. Oussoren, J. Zuidema, D. J. A. Crommelin, G. Storm, *Biochim. Biophys. Acta Biomembr.* **1997**, *1328*, 261 – 272.
[8] a) S. Kim, J. W. Park, D. Kim, D. Kim, I.-H. Lee, S. Jon, *Angew. Chem.* **2009**, *121*, 4202 – 4205; *Angew. Chem. Int. Ed.* **2009**, *48*, 4138 – 4141; b) S. K. Libutti, G. F. Paciotti, A. A. Byrnes, H. Richard Alexander Jr., W. E. Gannon, M. Walker, G. D. Seidel, N. Yuldasheva, L. Tamarkin, *Clin Cancer Res.* **2010**, *16*, 6139 – 6149; c) A. C. Powell, G. F. Paciotti, S. K. Libutti, *Methods Mol. Biol.* **2010**, *624*, 375 – 384; d) R. Goel, N. Shah, R. Visaria, G. F. Paciotti, J. C. Bischof, *Nanomedicine* **2009**, *4*, 401 – 410.
[9] N. G. Bastús, E. Sánchez-Tilló, S. Pujals, C. Farrera, C. López, E. Giralt, A. Celada, J. Lloberas, V. Puntes, *ACS Nano* **2009**, *3*, 1335 – 1344.
[10] D. Kim, Y. Y. Jeong, S. Jon, *ACS Nano* **2010**, *4*, 3689 – 3696.
[11] D. Kim, S. Park, J. H. Lee, Y. Y. Jeong, S. Jon, *J. Am. Chem. Soc.* **2007**, *129*, 2661 – 2665.
[12] D. Gabrilovich, *Methods Mol. Med.* **2001**, *64*, 3 – 7.
[13] a) R. S. Allan, J. Waithman, S. Bedoui, C. M. Jones, J. A. Villadangos, Y. Zhan, A. M. Lew, K. Shortman, W. R. Heath, F. R. Carbone, *Immunity* **2006**, *25*, 153 – 162; b) K. L. Knutson, M. L. Disis, *Cancer Immunol. Immunother.* **2005**, *54*, 721 – 728; c) E. Segura, J. A. Villadangos, *Curr. Opin. Immunol.* **2009**, *21*, 105 – 110; d) S. Hirosuea, I. C. Kourtisa, A. J. v. d. Vliesa, J. A. Hubbell, M. A. Swartz, *Vaccine* **2010**, *28*, 7897 – 7906; e) L. J. Cruz, F. Rueda, B. a. Cordobilla, L. Simón, L. Hosta, F. Albericio, J. C. Domingo, *Mol. Pharm.* **2011**, *8*, 104 – 116.
[14] A. Braun, T. Worbs, G. L. Moschovakis, S. Halle, K. Hoffmann, J. Bölter, A. Münk, R. Förster, *Nat. Immunol.* **2011**, *12*, 879 – 887.
[15] E. Harlow, D. Lane, *Antibodies: A Laboratory Manual*, CSHL, NY, **1988**, p. 99.
[16] H. Li, Y. Li, J. Jiao, H.-M. Hu, *Nat. Nanotechnol.* **2011**, *6*, 645 – 650.
[17] a) M. Kortylewski, M. Kujawski, A. Herrmann, C. Yang, L. Wang, Y. Liu, R. Salcedo, H. Yu, *Cancer Res.* **2009**, *69*, 2497 – 2505; b) J. Vollmer, A. M. Krieg, *Adv. Drug Delivery Rev.* **2009**, *61*, 195 – 204; c) J. Li, W. Song, D. K. Czerwinski, B. Varghese, S. Uematsu, S. Akira, A. M. Krieg, R. Levy, *J. Immunol.* **2007**, *179*, 2493 – 2500.
[18] a) I.-H. Lee, S. An, M. K. Yu, H.-K. Kwon, S.-H. Im, S. Jon, *J. Controlled Release* **2011**, *155*, 435 – 441; b) V. Bagalkot, I.-H. Lee, M. K. Yu, E. Lee, S. Park, J.-H. Lee, S. Jon, *Mol. Pharm.* **2009**, *6*, 1019 – 1028.
[19] a) W.-C. Chang, C.-H. Li, S.-C. Huang, D.-Y. Chang, L.-Y. Chou, B.-C. Sheu, *Cancer* **2010**, *116*, 5777 – 5788; b) S. F. Cai, T. A. Fehniger, X. Cao, J. C. Mayer, J. D. Brune, A. R. French, T. J. Ley, *J. Immunol.* **2009**, *182*, 6287 – 6297.
[20] A. Bolhassani, S. Safaiyan, S. Rafati, *Mol. Cancer* **2011**, *10*, 3.
[21] a) M. Feldmann, A. Basten, *J. Exp. Med.* **1971**, *134*, 103 – 119; b) R. Barrington, M. Zhang, M. Fischer, M. C. Carroll, *Immunol. Rev.* **2001**, *180*, 5 – 15.

  